Thermochimica Acta, 161 (1990) 327–337
Elsevier Science Publishers B.V., Amsterdam – Printed in The Netherlands

A THERMOGRAVIMETRIC STUDY OF THE REACTION BETWEEN SULFUR DIOXIDE AND CALCIUM OXIDE

S. GHARDASHKHANI and D.A. COOPER

Department of Inorganic Chemistry, Chalmers University of Technology and University of Göteborg, S-412 96 Göteborg (Sweden)

(Received 24 October 1989)

ABSTRACT

The reaction between sulfur dioxide and calcium oxide, pertaining to atmospheric fluidized bed combustion, was investigated using thermogravimetric analysis, IR spectroscopy and X-ray powder diffraction, at 600–900 °C and with SO_2 concentrations of 0.1–0.9% in N_2. The reaction was observed to have a non-zero SO_2 reaction order, and in general the rate of reaction decreased with increasing temperature; $CaSO_4$, $CaSO_3$ and CaS were identified as reaction products, and a consecutive reaction mechanism is proposed with $CaSO_3$ as a key intermediate.

INTRODUCTION

The application of calcium-based sorbents, such as limestone or dolomite, in fluidized bed coal combustion to reduce sulfur dioxide emissions is a well established technique. In this case the calcium introduced into the fluidized bed boiler is in the form of calcium carbonate ($CaCO_3$). Within the temperature range of interest, 700–950 °C, the carbonate is rapidly calcined to the porous oxide (CaO), which can subsequently react with SO_2 to form calcium sulfate ($CaSO_4$).

Numerous experimental studies in laboratory-sized reactors have been undertaken, examining the sulfation reaction under varying oxidizing conditions pertaining to the fluidized bed boiler environment [1–6]. It has been suggested that a possible mechanism in the sulfation reaction could be SO_2 interaction with CaO, as described in eqn. (1), followed by a subsequent disproportionation of $CaSO_3$ as in eqn. (2) [4,5]. The CaS fraction formed in eqn. (2) can then readily be oxidized to give additional $CaSO_4$

$$CaO(s) + SO_2(g) \rightleftharpoons CaSO_3(s) \quad (1)$$

$$4CaSO_3(s) \rightleftharpoons 3CaSO_4(s) + CaS(s) \quad (2)$$

Further experiments, specifically directed at studying the reactions of eqns. (1) and (2), have so far been restricted to using crystalline $CaSO_3$ samples

0040-6031/90/$03.50

[7–11] and relatively high SO_2 concentrations [12,13] at temperatures often outside those relevant to fluidized bed combustion. Consequently, the purpose of this investigation was to study the interaction of SO_2 and CaO with a view to verifying the possible occurrence of reactions (1) and (2) at conditions more appropriate to the fluidized bed application.

EXPERIMENTAL

Reagent grade $CaCO_3$ (Merck, 99%) with particle sizes ranging from 10–50 μm was used to prepare CaO. High purity sulfur dioxide (2% SO_2 in N_2), nitrogen and carbon monoxide were employed, and the desired gas mixtures were obtained by adjusting the appropriate flow rates using precalibrated rotameters. The reaction progress was followed by thermogravimetric (TG) analysis (Mettler TA1 apparatus with a middle range quartz furnace and controlled atmosphere accessory), where the balance housing was protected by a nitrogen purge during all experiments. A platinum–platinum, 10% rhodium standard thermocouple was used to measure the temperature near the reaction site, below a platinum hemispherical crucible sample holder (diameter 15 mm, depth 10 mm). Samples of $CaCO_3$ were placed centrally in the sample holder for each run. The reaction's solid products were analyzed by X-ray powder diffraction (XRD, Huber vertical Guinier camera 620) and Fourier transform infrared spectroscopy (FTIR, Mattson Polaris FTIR system) using the KBr-pellet technique. The BET specific surface area of the calcined sample (CaO) was measured by nitrogen adsorption as ca. 10 $m^2\ g^{-1}$ (Digisorb 2600 apparatus).

Procedure

Calcium oxide (CaO) was prepared by calcining a preweighed sample of $CaCO_3$ under nitrogen (flow rate 200 ml min^{-1} at 25 °C) in the TG apparatus. Heating of the furnace was performed at a rate of 25 °C min^{-1} up to 850 °C, at which temperature virtually complete calcination was achieved, and the amount of CaO present in each sample was determined from the total weight loss measured. At this point the temperature of the furnace was re-set to the desired sulfation reaction temperature (heating or cooling rate of 25 °C min^{-1}) and, when temperature equilibration was observed, the atmosphere was changed from nitrogen (previously adjusted to 600 ml min^{-1}) to the reacting gas mixture (600 ml min^{-1}) using two three-way cross valves. The reaction time was 120 min for all experiments.

At the end of the reaction time, a number of samples were allowed to cool to ambient temperature under nitrogen at an average cooling rate of 100 °C min^{-1}. It should be noted that, to prevent further product formation, any traces of SO_2 remaining in the system were removed by flushing with

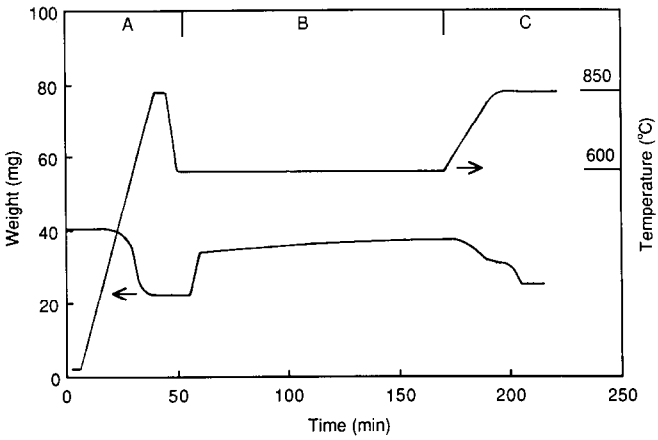

Fig. 1. TG diagram for the experiment at 600 °C with 0.3% SO_2 (N_2 making up the balance): A, calcination step, B, reaction between SO_2 and CaO, and C, reduction step using 100% CO.

nitrogen for 1 min before the cooling period. The samples were then removed from the TG apparatus and degassed at a pressure of ca. 10^{-6} atm for 10 min in an evacuation chamber. Subsequently, the evacuation chamber was filled with nitrogen and the samples were promptly analyzed by FTIR (KBr pellets pressed at 350 kg cm^{-2}) and XRD.

In other experiments after the 120 min reaction time, the amount of $CaSO_4/CaSO_3$ present could be determined through weight changes (corrected for buoyancy effect) by reducing the products to CaS using 100% CO (flow rate 200 ml min^{-1}) at a temperature of 850 °C (any temperature adjustment being effected at a heating or cooling rate of 10 °C min^{-1}). The sensitivity of this method was checked by comparing experiments with pro analysi $CaSO_4$, where the reduction commenced at 760–770 °C [14], and with the products of the reaction obtained at 600 °C, where the sulfite reduction appeared at ca. 610–620 °C.

RESULTS

A typical TG diagram, weight/temperature against time, for the experiment carried out at a reaction temperature of 600 °C with 0.3% SO_2 (the remainder being N_2) is shown in Fig. 1. Stage A, characterized by weight loss, corresponds to the calcination of $CaCO_3$, stage B relates to the reaction between SO_2 and CaO, and stage C shows weight loss through the reduction of the formed $CaSO_4/CaSO_3$. It should be noted that stage C could be observed as a multistep reduction for the products formed at < 750 °C; the first, low temperature, reduction step presumably accounts for the $CaSO_3$

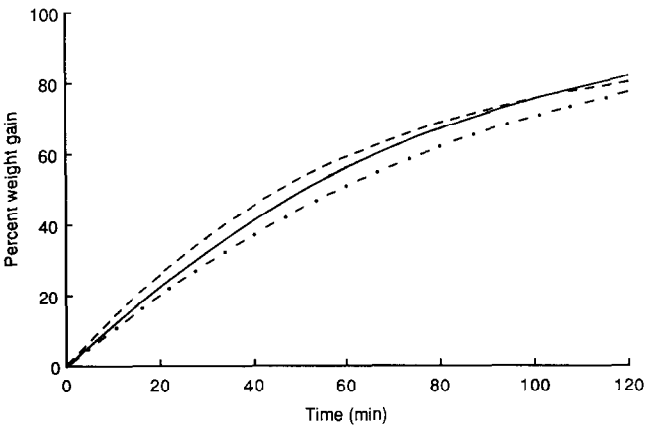

Fig. 2. Effect of different sample weights on rate of reaction at 800 °C with 0.3% SO_2 in N_2: — — —, 22 mg; ———, 44 mg; – · –, 66 mg.

conversion [eqn. (3)] and the secondary, higher temperature, reduction step for the $CaSO_4$ conversion [eqn. (4)].

$$CaSO_3(s) + 3CO(g) \rightleftharpoons CaS(s) + 3CO_2(g) \quad (3)$$

$$CaSO_4(s) + 4CO(g) \rightleftharpoons CaS(s) + 4CO_2(g) \quad (4)$$

For the experiments performed at a reaction temperature > 750 °C, it was evident that only trace amounts of $CaSO_3$ existed in the product, and thus in these cases no clear step-wise reduction was observed.

The TG data reported in Figs. 2, 3 and 4 are in terms of the percent weight gain, which refers to the weight gain per initial amount of CaO present in each sample. Although this treatment gives an overall measure of the reactions taking place, it should be borne in mind that the rates discussed below refer to a weight gain and not a molecular conversion, since differing fractions of $CaSO_4$, $CaSO_3$ and CaS exist in the products.

The effect of different sample weights on the rate of reaction with 0.3% SO_2 in N_2 at 800 °C is illustrated in Fig. 2, where the weights given are in terms of the CaO present in each sample after calcination. A small effect on the rate of reaction was observed, with the initial rate slightly greater for smaller sample weights. This phenomenon appears to be due to mass transfer resistance, i.e. slower inter-particular SO_2 penetration through the large samples to the underlying layers. A standard sample weight of 22 mg was used for all other experiments.

In Fig. 3, the influence of the SO_2 concentration in N_2 on the rate of reaction at 800 °C is presented. The rate was observed to increase successively with increasing SO_2 concentration, although for 0.6% and 0.9% SO_2 the rates markedly fall off after a comparatively rapid initial reaction. It seems probable that the initial fast rate of reaction occurs at the outer

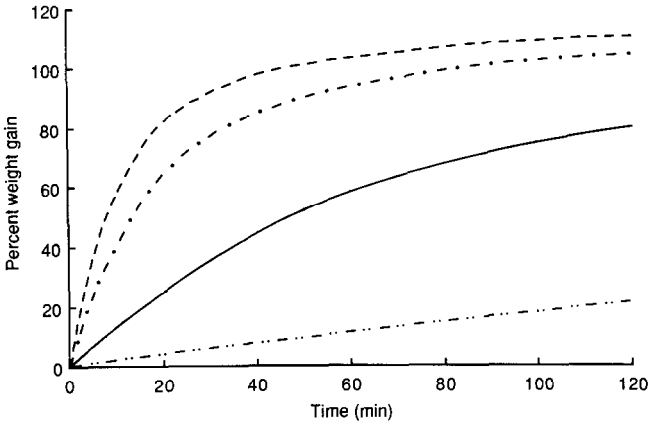

Fig. 3. Effect of SO_2 concentration on rate of reaction at 800 °C: –·–, 0.1% SO_2; ——, 0.3% SO_2; –·–, 0.6% SO_2; — — —, 0.9% SO_2.

surface and the subsequent slower reaction is due to the slow diffusion of SO_2 through the newly formed product layer.

The effect of temperature on the rate of reaction with 0.3% SO_2 in N_2 is shown in Fig. 4. The fastest rate was observed at 650 °C and, in general, increasing the temperature corresponded to a decrease in the rate (see Discussion section).

IR spectra

In Fig. 5, traces B–E show IR spectra obtained from similar experiments with 0.3% SO_2 in N_2, while trace A represents the spectrum of calcined

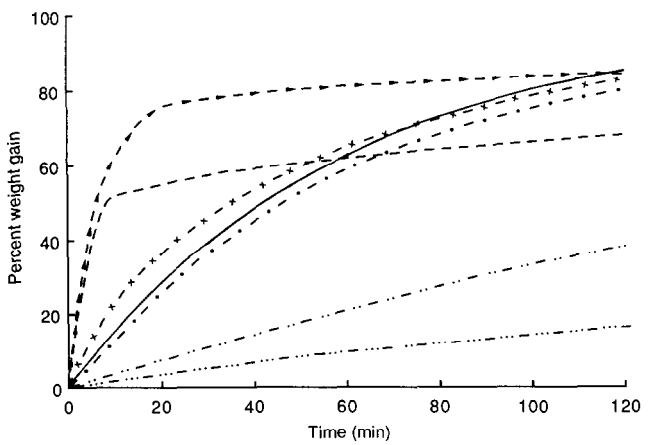

Fig. 4. Effect of temperature on rate of reaction with 0.3% SO_2 in N_2: – — —, 600 °C; –▶–, 650 °C; –×–, 700 °C; ——, 750 °C; –·–, 800 °C; –··–, 850 °C; –···–, 900 °C.

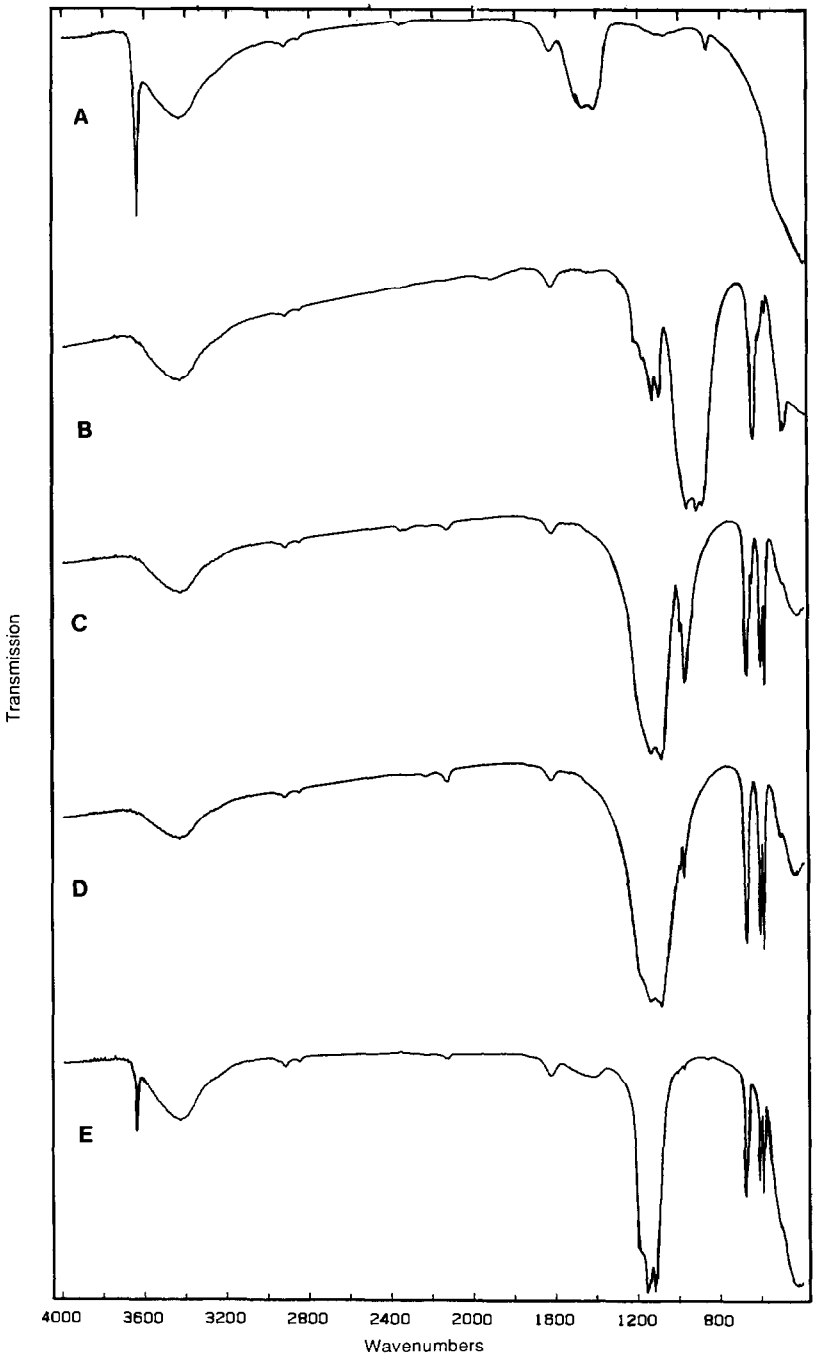

Fig. 5. IR spectra (wavenumbers in cm^{-1}) of calcined $CaCO_3$ (A) and of the products from experiments with 0.3% SO_2 in N_2: B, at 600 °C; C, at 700 °C; D, at 800 °C; E, at 900 °C.

$CaCO_3$ prior to sulfation. The broad band at 3200–3800 cm^{-1} of traces A–E is due to H_2O, which was incorporated into the KBr pellet matrix material, and the sharp band at 3650 cm^{-1} (traces A and E) would appear to be a result of $Ca(OH)_2$ [15] formed during sample preparation. In addition, despite TG weight stabilization to that expected for complete calcination, spectrum A also shows a band characteristic of residual CO_3^{2-}, at 1400 cm^{-1}, which could possibly originate from the adsorption of CO_2 from the air during the IR analysis. Trace B shows the spectrum of the product from the experiment run at 600 °C. The strong bands between 900–974 cm^{-1}, 657 cm^{-1} and 495 cm^{-1} are characteristic for SO_3^{2-} ($CaSO_3$) and the additional bands observed at 1090–1140 cm^{-1} correspond to SO_4^{2-} frequencies ($CaSO_4$) [15–18]. Trace C shows the IR spectrum of the product formed at 700 °C. In comparison to trace B, a decrease in intensity of the 972 cm^{-1} sulfite band and several subtle changes in the 600–700 cm^{-1} region of the spectrum are observed, together with more intense sulfate bands at 1090, 1140, 595, 612 and 676 cm^{-1}. This tendency of weakened sulfite and strengthened sulfate band frequencies with increased reaction temperature is also reflected in trace D. In trace E (reaction at 900 °C) the sulfite bands are absent and the spectrum is consistent with a $CaSO_4$ product. Interestingly, the OH band at 3650 cm^{-1} originating from $Ca(OH)_2$ reappears in trace E, which suggests the presence of some unreacted CaO and thus a relatively slow reaction at this temperature.

Table 1 summarizes the principal results of the analyses (TG, XRD and FTIR) and the experimental scope of this investigation. In general, consistent product identifications for each experiment were obtained. It should be noted that XRD analyses allow the detection of all possible Ca species, whereas only $CaSO_3$, $CaSO_4$ and $Ca(OH)_2$ could be seen with FTIR (over

TABLE 1

Summary of experimental results as determined by TG, XRD and FTIR

SO_2 (%)	Temperature (°C)	Sulfur distribution determined by TG (mol%)			Phase identification	
		$CaSO_4$	$CaSO_3$	CaS	XRD	FTIR
0.3	600	13	18	0	$CaSO_4$, $CaSO_3$, CaO	$CaSO_3$, $CaSO_4$
0.3	650	21	15	0		
0.3	700	32	2	7	$CaSO_4$, CaS, CaO	$CaSO_3$, $CaSO_4$
0.3	750	34	0	11		
0.3	800	32	0	10	$CaSO_4$, CaS, CaO	$CaSO_3$, $CaSO_4$
0.3	850	16	0	2		
0.3	900	7	0	0	$CaSO_4$, CaO, $Ca(OH)_2$	$CaSO_4$, $Ca(OH)_2$
0.1	800	9	0	0	–	–
0.6	800	42	0	11	–	–
0.9	800	44	0	7	$CaSO_4$, CaS, CaO	$CaSO_3$, $CaSO_4$

the frequency range of this study). The latter, however, has a greater sensitivity, and thus the $CaSO_3$ present in the product at 700 and 800 °C was observed only by FTIR and could not be inferred from TG or XRD.

DISCUSSION

As indicated by Fig. 2, the experiments conducted appear to be subject to mass transfer resistance, and thus a detailed kinetic study of this reaction system was not possible. Although temperature influences this effect slightly, the identical sample weights and gas flow rates used do, however, allow some qualitative comparison between the reaction rates to be made.

A reasonable interpretation of the results can be accounted for by assuming a consecutive reaction mechanism consisting of eqns. (1) and (2), with $CaSO_3$ as the key intermediate. From thermodynamic data [19] both steps are exothermic up to at least 750 °C [20], while the magnitude of the Gibbs free energy change (proportional to the logarithm of the equilibrium constant, $\Delta G = -RT \ln K$) of the disproportionation (eqn. (2)) decreases somewhat more slowly with increasing temperature than that for the sulfation [21]. That is,

$$\frac{dK_1(T)}{dT} > \frac{dK_2(T)}{dT}$$

over the temperature range of interest. To avoid complications with fractional reaction orders we consider the simplified consecutive mechanism

$$\mathrm{R} \underset{k_{-1}}{\overset{k_1}{\rightleftarrows}} \mathrm{X} \underset{k_{-2}}{\overset{k_2}{\rightleftarrows}} \mathrm{P}$$

where reactant R progresses through the intermediate X and then on to product P. The corresponding equilibrium constants can be expressed in terms of the elementary rate coefficients as follows

$$K_1(T) = \frac{k_1(T)}{k_{-1}(T)}, \qquad K_2(T) = \frac{k_2(T)}{k_{-2}(T)}$$

By invoking a steady-state assumption on the formation rate of the intermediate X, we easily obtain the rate of product appearance

$$\frac{d}{dt}[\mathrm{P}] = -\frac{d}{dt}[\mathrm{R}] = \frac{1}{k_{-1} + k_2}(k_1 k_2[\mathrm{R}] - k_{-1}k_{-2}[\mathrm{P}])$$

$$= \frac{k_{-2}}{(k_{-2}K_1)/k_{-1} + (K_1/K_2)}\left(K_1^2[\mathrm{R}] - \frac{K_1}{K_2}[\mathrm{P}]\right)$$

$$= \frac{k_{-2}}{(k_2K_2)/k_1 + (K_2/K_1)}\left(K_2^2[\mathrm{R}] - \frac{K_2}{K_1}[\mathrm{P}]\right)$$

In the limit of high temperature such that K_1/K_2 becomes vanishingly small, this rate becomes

$$T \to \infty \Rightarrow \frac{K_1}{K_2} \to 0 \Rightarrow \frac{\mathrm{d}}{\mathrm{d}t}[\mathrm{P}] \to k_1[\mathrm{R}]$$

Similarly, in the low temperature asymptote, the initial step is also rate determining at short times

$$T \to 0 \Rightarrow \frac{K_2}{K_1} \to 0 \Rightarrow \frac{\mathrm{d}}{\mathrm{d}t}[\mathrm{P}] \to k_1[\mathrm{R}]$$

At both these limits the elementary rate coefficient, and hence the overall rate, will increase with temperature. In the intermediate regime, however, there exists a temperature $T^\star$ such that the ratio of equilibrium constants is unity, i.e. $K_1 = K_2 = K$, say. Here we have

$$T \to T^\star \Rightarrow \frac{K_1}{K_2} \to 1 \Rightarrow \frac{\mathrm{d}}{\mathrm{d}t}[\mathrm{P}] \to \left(\frac{K}{K + k_1/k_2}\right) k_1[\mathrm{R}]$$

at short times, where it is assumed that no product P is initially present. The additional factor is manifestly less than unity, and is particularly small if $k_1 \gg k_2$, when the second step controls the overall rate. Under such circumstances, the overall rate will pass through a maximum about the temperature $T^\star$. The observed temperature characteristic of the $CaSO_4$ production rate in the CaO–SO_2 system is consistent with this simplified model where we can specify the transition temperature $T^\star$ in the range 600–700 °C. Furthermore, calculations from thermodynamic tables indicate also that $K_1/K_2 \approx 0.7$ at 1000 K [19].

Further support for the proposed mechanism is evident from the experiments conducted with varying SO_2 concentrations. Fig. 3 is clearly indicative of a non-zero SO_2 reaction order, and a simultaneous strengthening of the sulfite bands was observed in the FTIR spectra with increased SO_2 concentrations (0.3–0.9%). A detailed account of the kinetics, however, would require a more sophisticated mechanism than that proposed above, where for example, the heterogeneous surface reaction (eqn. (1)) and subsequent migration of products by homogeneous disproportionation (eqn. (2)) through the CaO particle are considered explicitly in terms of active surface sites.

For the most part, the sulfur species distribution in Table 1 is in accordance with the consecutive mechanism of eqns. (1) and (2). Reaction (1) predominates at low temperatures but reaction (2) becomes increasingly important at higher temperatures, and thus a build-up of $CaSO_4$ and CaS occurs at the expense of $CaSO_3$ with increasing temperature. Since eqn. (1), and hence $CaSO_3$ formation, is limited at elevated temperatures, however, $CaSO_4$ and CaS production via reaction (2) also subsequently falls. In addition, the disproportionation of $CaSO_3$ (eqn. (2)) is known to begin at ca. 660–680 °C in an inert atmosphere [8,10], which could account for the

absence of CaS at 600–650 °C (Table 1). Interestingly the $CaSO_4$: CaS mole ratios reported in Table 1 are not constant, as would be expected on the basis of the mechanism of only eqns. (1) and (2). The absence of CaS at high temperatures can possibly be attributed to its oxidation by SO_2 as in eqn. (5) [12], while at temperatures < 700 °C the oxidation of $CaSO_3$ (eqn. (6)) is believed to predominate over the disproportionation reaction (1) [12,22].

$$CaS(s) + 2SO_2(g) \rightleftharpoons CaSO_4(s) + S_2(g) \quad (5)$$

$$2CaSO_3(s) + SO_2(g) \rightleftharpoons 2CaSO_4(s) + \tfrac{1}{2}S_2(g) \quad (6)$$

The elemental sulfur product, however, as predicted by eqns. (5) and (6), was not detected, either visually or by XRD, in the present study.

Although oxidizing, reducing and inert environments are inherent in fluidized bed combustion, it should be stressed that this study has been restricted to examining the reaction of CaO and SO_2 under inert conditions. According to previous investigations, the presence of oxygen would allow the formation of $CaSO_4$, while reducing conditions (CO) would lead to solely CaS as the Ca-containing species. In the present investigation, the results clearly suggest the existence of a $CaSO_3$ intermediate via eqn. (1), but the question remains as to whether this primary reaction is prevalent under all fluidized bed combustion conditions. Some support for this proposal may lie in the temperature dependence of SO_2 removal found in operating boilers [23], which is consistent with that observed in the present study.

ACKNOWLEDGEMENTS

We express our gratitude to the Swedish National Energy Administration for financial support and to Claes Tullin, Robert Penfold, Dr. Claire Adenis and Professor Oliver Lindqvist for helpful discussions.

REFERENCES

1 R.H. Borgwardt, Environ. Sci. Technol., 4 (1) (1970) 23.
2 R.H. Borgwardt and R.D. Harvey, Environ. Sci. Technol., 6 (4) (1972) 350.
3 R.H. Borgwardt and R. Bruce, AIChE J., 32 (2) (1986) 239.
4 R.W. Coutant, R.E. Barrett and E.H. Lougher, J. Eng. Power, 92 (2) (1970) 113.
5 E.P. O'Neill, D.L. Keairns and W.F. Kittle, Thermochim. Acta, 14 (1976) 209.
6 J.S. Dennis and A.N. Hayhurst, Proc. 20th Symp. (Int.) on Combustion, Inst. of Combustion, Pittsburg, 1985 p. 1347.
7 F. Foerster and K. Kuble, Z. Anorg. Chem., 139 (1924) 261.
8 T.R. Ingraham and P. Marier, J. Air Pollut. Control Assoc., 21 (6) (1971) 347.
9 D.R. Glasson and P. O'Neill, Proc. 1st Eur. Symp. Therm. Anal., Heyden, London, 1976, p. 283.
10 R. Matsuzaki, H. Masumizu, N. Murakami and Y. Saeki, Bull. Chem. Soc. Jpn., 51 (1) (1978) 121.

11 L.O. Ferguson and E.F. Rissman, Proc. 2nd Int. Clean Air Congr., Academic Press, New York, 1971, p. 753.
12 A.N. Ketov, V.V. Pechkovskii, J. Appl. Chem. USSR, 31 (7) (1958) 1774.
13 A.N. Ketov, V.V. Pechkovskii, and V.V. Larikov, J. Appl. Chem. USSR, 44 (7) (1971) 1640.
14 R. Kuusik, P. Saikkonen and L. Niinistö, J. Therm. Anal., 30 (1987) 187.
15 K. Nakamoto, Infrared and Raman Spectra of Inorganic and Coordination Compounds, Wiley, New York, 4th edn., 1986.
16 M.J.D. Low, A.J. Goodsel and N. Takezawa, Environ. Sci. Technol., 5 (12) (1971) 1191.
17 M. Mega, J.W. Childers and R.A. Palmer, Appl. Spectrosc., 41 (1) (1987) 120.
18 H.D. Lutz and S. Elsuradi, Z. Anorg. Allg. Chem., 425 (1976) 134.
19 I. Barin, O. Knacke and O. Kubaschewski, Thermochemical Properties of Inorganic Substances, Supplement, Springer, Berlin, 1977.
20 J. Tarradellas and L. Bonnetain, Bull. Soc. Chim. Fr., 6 (1973) 1903.
21 K. Schwitzgeble and P.S. Lowell, Environ. Sci. Technol., 7 (13) (1973) 1147.
22 G. van Houte and B. Delmon, Bull. Soc. Chim. Belg., 87 (4) (1978) 241.
23 A. Lyngfelt, Thesis, Chalmers University of Technology, Göteborg, 1988.